2022-12

The spatial extent of magnetopause magnetic reconnection from in situ THE...

JGR Space Physics

RESEARCH ARTICLE
10.1029/2022JA030894

Special Section:
Fifteen Years of THEMIS Mission

The Spatial Extent of Magnetopause Magnetic Reconnection From In Situ THEMIS Measurements

Emil A. Atz[1], Brian M. Walsh[1], Jef M. Broll[2], and Ying Zou[3]

[1]College of Engineering and Center for Space Physics, Boston University, Boston, MA, USA, [2]Los Alamos National Laboratory, Space Sciences and Applications Group, Los Alamos, NM, USA, [3]University of Alabama, Huntsville, AL, USA

Key Points:

- THEMIS conjunction observations at the magnetopause are used to determine the spatial extent of magnetopause reconnection
- Two spacecraft are more likely to both observe reconnection jets the closer they are spatially
- Diamagnetic suppression is a reason why reconnection at the magnetopause is not always spatially extended

Correspondence to:
E. A. Atz,
emilatz@bu.edu

Citation:
Atz, E. A., Walsh, B. M., Broll, J. M., & Zou, Y. (2022). The spatial extent of magnetopause magnetic reconnection from in situ THEMIS measurements. *Journal of Geophysical Research: Space Physics*, *127*, e2022JA030894. https://doi.org/10.1029/2022JA030894

Received 2 AUG 2022
Accepted 9 DEC 2022

Abstract Magnetic reconnection at the magnetopause has long been studied with multi-spacecraft observations. In this work, data from the five satellite THEMIS mission during the years of 2008–2010 are used to generate statistics regarding the spatial extent of magnetopause reconnection. The presence of a reconnecting magnetopause is determined with the Walén relation as two satellites cross the magnetopause simultaneously. In some cases both satellites measure reconnection whereas in others one satellite measures reconnection and the other does not. This study finds that two spacecraft are more likely to observe a contiguous reconnection region the closer they are spatially, and that reconnection is not always extended around the entire magnetopause. Plasma β gradient drifts are investigated as a cause of local reconnection suppression. Spacecraft position along the magnetopause flanks is also investigated as a possible spatial limitation to reconnection due to changes in shear flow or boundary thickness.

Plain Language Summary Magnetic reconnection, a process by which magnetic fields break and reform, is observed with the THEMIS satellites at Earth's magnetopause. Using two satellites crossing the magnetopause near simultaneously, the spatial extent of reconnection can be sampled. This study found 208 of these such events from 2008 to 2010, and find that simultaneous reconnection is more likely to be measured the closer satellites spatially are. We additionally conclude that reconnection is not always extended around the magnetopause because events are found in which only one satellite observes reconnection. We explore the possible causes of reconnection confinement with analysis of the magnetic field shear angle and plasma beta, as well as spacecraft position along the magnetopause flanks.

1. Introduction

The magnetopause serves as the boundary between Earth's plasma and magnetic field environment and the shocked solar wind. The magnetopause is a dynamic magnetic and plasma discontinuity where energy is transferred between the interplanetary magnetic field and magnetosphere (Lyon, 2000). One mechanism of energy transfer is by magnetic reconnection, in which magnetic fields (in this case solar wind and magnetospheric) break and rearrange in three dimensions. The line along which the magnetic fields reconnect is known as the X-line or a reconnecting separator. The length scale of the X-line along the magnetopause is critical to predict the global efficiency and quantity of energy transfer into the magnetosphere.

As a result of magnetic reconnection, the reconfiguration of the magnetic fields produces an exhaust, or jet, originating from the X-line. The jet is a rapid flow of plasma tangential to the magnetopause. A spacecraft observation of a jet is an indication that reconnection is occurring near-by along the magnetic field lines the spacecraft is crossing. Observations of the jet are quantifiable evidence of reconnection at the given local time (LT) the satellite crosses the magnetopause (e.g., Fuselier et al. (1991)).

Multi-spacecraft observations can be utilized when estimating the length of the X-line. When two spacecraft observe reconnection near simultaneously when crossing the magnetopause, the length of the X-line is inferred as the distance between the spacecraft. Study of magnetopause reconnection varies greatly in scale.

Observations with the five satellite Magnetospheric Multi-Scale (MMS) mission focus on the small region (10's of kilometers) where reconnection initiates, known as the diffusion region (e.g., Burch and Phan (2016); Eriksson et al. (2016); L.-J. Chen et al. (2016); K. Genestreti et al. (2017); K. J. Genestreti et al. (2018)). The small target of the MMS mission, the diffusion region, is extremely challenging to sample (Fuselier et al., 2017). At larger scales, multi-spacecraft observations of the jet exhaust of magnetic reconnection are more common.

At larger scales than MMS observations, measurements with spacecraft separated by a few to many Earth radii (Re) from missions like Cluster, THEMIS and others, have confirmed instances of extended magnetopause reconnection (e.g., Phan et al. (2000); Fear et al. (2010); Dunlop et al. (2011); Walsh et al. (2014)) but also localized patches (e.g., Sandholt and Farrugia (2003); Trattner et al. (2005); Fear et al. (2010); Walsh et al. (2017); Zou et al. (2019, 2020)). One possibility to explain the conflicting experimental measurements is the spreading and merging of X-lines.

Modeling of the magnetopause can provide necessary context with global, time continuous results. Models such as that employed by Shay et al. (2003) using a two fluid model, and that used by Y. Chen et al. (2020) using a magnetohydrodynamic (MHD) with embedded particle-in-cell (PIC) model found localized X-line patches spreading and becoming more extended. The process of spreading is commonly observed in models and has been the focus of a dedicated study by Li et al. (2020). Sun et al. (2019), in a global MHD model, present reconnection occurring at variable length scales (<1 to >10 Re) of flux transfer events, rapid instances of magnetic reconnection. Additionally, Hoilijoki et al. (2017) in a global hybrid-Vlasov simulation show spatial and temporal reconnection variability even when solar wind conditions are constant. With many model types, reconnection models show dynamics in time and space.

Another method of studying magnetopause reconnection is with auroral and radar measurements from high latitudes (Chisham et al., 2008; Frey et al., 2019). Ground-based observations rely on energy transported along reconnected magnetic field lines into the ionosphere where enhanced plasma flows indicate the location and size of the X-line. This observation method has shown broad X-line length at the magnetopause (Fuselier et al., 2002; Milan et al., 2000; Pinnock et al., 2003), but also variability in X-line length (Zou et al., 2019). Ground observations can also be used to determine X-line spreading speeds (Zou et al., 2018).

Although single event observations are useful moments in time to study, generalized spatial reconnection properties require statistics. Ionospheric signatures can be challenging to produce conclusive magnetopause reconnection properties (e.g., Petrinec and Fuselier (2003)). Multi-spacecraft observations require years of statistics due to the limitations of orbits. With a large data set of multiple satellites at the magnetopause, spatial reconnection properties can be probed.

THEMIS, a five-spacecraft mission equipped with plasma and magnetic field instruments, has been passing through the magnetopause since 2007 (Angelopoulos, 2009). Magnetic field data from the fluxgate magnetometer (FGM) (Auster et al., 2008) and plasma moments, including velocity and density, from the electrostatic analyzer (ESA) (McFadden et al., 2008) on board the THEMIS spacecraft are used for analyzing a magnetopause crossing.

THEMIS magnetopause conjunction crossings, or events, are when two THEMIS spacecraft cross the magnetopause simultaneously. We present a statistical analysis of these magnetopause measurements, providing X-line observations ranging from fractions of Re to more than 12 Re in satellite spacing. The results show that reconnection is not always extended, and that spacecraft are more likely to both observe reconnection the closer they are. We also explore two mechanisms by which reconnection can be limited. Gradients in plasma β and magnetic shear ($\Delta\beta$–θ relationship described in Section 4) as well as location along the magnetopause flank (described in Section 5) may play a role in limiting the spatial extent of reconnection.

2. Analysis Methods

2.1. Database

This work summarizes uses years 2008–2010 of THEMIS observations of the magnetopause with focus on the occurrence of magnetic reconnection observed by two spacecraft crossing the magnetopause simultaneously. A handful of previous studies have presented a single case study or a small number of multi-spacecraft conjunctions. Here, the work systematically focuses on these time periods to define the meso- and macro-scale physics. During 2008–2010, the spacecraft orbits precessed in LT and experienced a range of inter-spacecraft spacing along the orbit. This enabled various inter-spacecraft spacing during magnetopause conjunctions. In later years, the spacecraft positions were maintained in a tighter orbit pattern, which limited the variability of spacecraft spacing.

The first step of generating a database of multi-spacecraft magnetopause conjunctions is to find instances of individual spacecraft magnetopause crossings. Possible crossings were found by identifying spikes in the standard deviation of the geocentric solar magnetic coordinate system (GSM) Z component, Bz, in a moving window, as

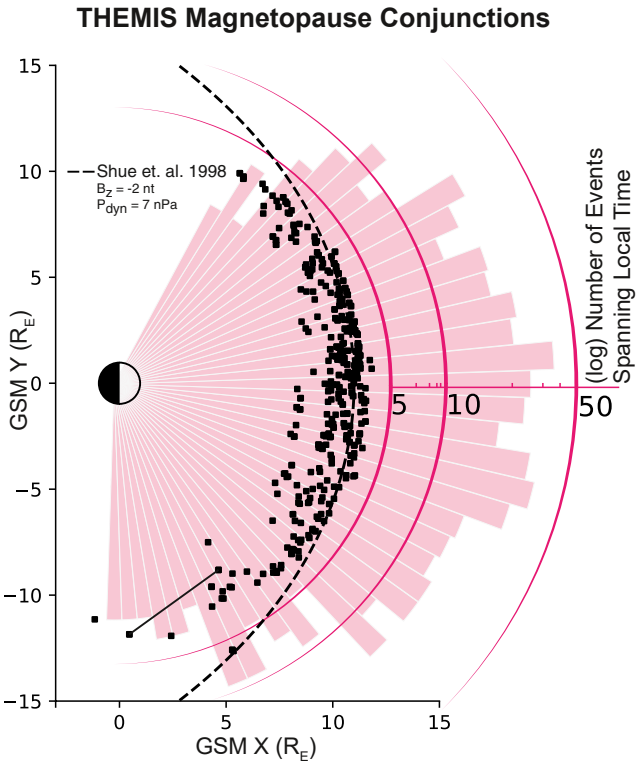

Figure 1. Magnetopause distribution of THEMIS spacecraft observations used in this analysis. Black squares are individual spacecraft locations when the magnetopause is observed. Dashed line is a representative magnetopause model from Shue et al. (1998). Pink bars, in log scale, (width of 15 min in local time (LT)) count the LT extent of the inter-spacecraft spacing for each conjunction event. The two spacecraft locations connected by a black line show one example of a conjunction LT extent. A count is added to each bin that the black line crosses.

well as visual inspection of Bz data. The times of these possible crossings are then compared between spacecraft. When a crossing of multiple spacecraft was within 15 min of each other, the magnetic field, plasma velocity, density and ion energy flux for each spacecraft were plotted. This potential conjunction was then analyzed further for confirmation of a conjunction event.

The Walén relation was applied to the data if; both spacecraft crossed the magnetopause at a similar time (≤5 min, selected to account for spreading speeds discussed in Section 2.2), there were no data gaps, and no large variability of necessary Walén relation parameters (e.g., magnetic field, density, plasma velocity, anisotropy factor). The Walén relation was applied to 208 conjunction events. The positions of the satellites and LT extent of the conjunctions covered the entire dayside magnetopause. Figure 1 is a combination of two plots. The individual spacecraft positions are shown in black squares, and the pink bar plot summarizes the LT extent of the inter-spacecraft spacing for each conjunction event. An example LT extent of a conjunction is shown with the two connected satellite locations. The pink bars are each 15 min wide in LT. The histogram shows that a majority of observations have a LT extent near the sub-solar region.

In this paper, measurement of "length" only considered the Euclidean distance between the satellites during a conjunction. A magnetopause model would be required to estimate the curved distance along the magnetopause between the satellites. This model would require additional assumptions that would make statistical comparison more challenging and dependent on the magnetopause model. Satellite spacing of the events ranged from hundreds of kilometers to more than 12 Re (Figure 2 in pink with 208 events). Statistical analysis, Section 3, only consists of events below 8,000 km due to low statistics of conjunction events larger than 8,000 km (Figure 2 in blue). The 174 events below 8,000 km have a mean value of 3,540 km. The impact of instabilities such as plasma β drifts on the extent of reconnection is investigated in this study for the collection of events with good sampling coverage at a spacing less than 8,000 km. For conjunctions with large inter-spacecraft spacing (>8,000 km), the impact of distance from the subsolar point on reconnection length is investigated.

2.2. Event Processing Method

For analysis of a magnetopause crossing, magnetic field and plasma data are interpolated linearly to match a 3 s frequency. A crossing is analyzed for the presence of a reconnection jet with the Walén relation.

The relation is a comparison of the observed and theoretical plasma jet velocities. The Walén relation developed by Hudson (1970), Paschmann et al. (1979) and Sonnerup et al. (1981) and later elaborated on by Paschmann et al. (1986), Trenchi et al. (2008), Phan et al. (2013) provides the theoretical velocity enhancements at regions of magnetic discontinuity. The spacecraft measurements provide the observed. The Walén relation assumes a 1-D rotational discontinuity (the magnetic field rotates around one axis across the boundary). A high level of agreement of the theoretical to the observed plasma jet velocity and direction provides quantitative evidence of a reconnecting magnetopause during the crossing.

The theoretical plasma velocity enhancement (the reconnection jet) is calculated as follows:

$$\Delta\vec{V}_{theoretical} = \pm\left(\frac{1-\alpha_1}{\mu_0\rho_1}\right)^{(1/2)}\left[\vec{B}_2\left(\frac{1-\alpha_2}{1-\alpha_1}\right)-\vec{B}_1\right] \quad (1)$$

where

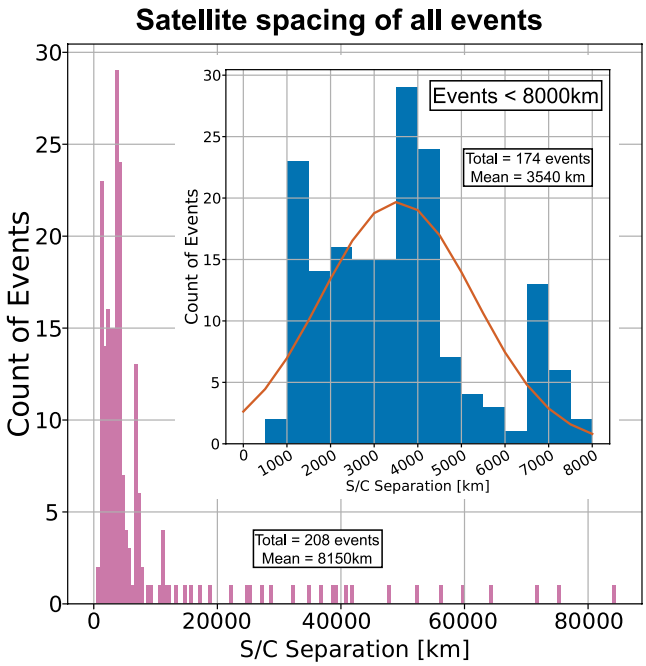

Figure 2. Histograms of the satellite spacing for conjunction events. Pink shows all events and blue shows events below 8,000 km spacing. A Gaussian fit to each data set is shown in the orange line.

$$\alpha = (P_{\parallel} - P_{\perp})\,\mu_0/\vec{B}^2 \tag{2}$$

In these equations, $\vec{B}$ is the magnetic field vector, and ρ is the plasma mass density, assuming a quasi-neutral plasma state. μ_0 is the vacuum permeability and α is the anisotropy factor. $P_{\parallel}$ and $P_{\perp}$ are the plasma pressures in the parallel and perpendicular directions to the magnetic field. $\Delta\vec{V}_{theoretical}$ is evaluated at each data point across a window that captures the magnetopause crossing in the instrument data. Subscript 1 is the magnetosheath reference data point. The value of the magnetosheath reference point is constant for each step of $\Delta\vec{V}_{theoretical}$. Subscript 2 is each data point inside the window of the data that spans the magnetopause (stepped through in the analysis as the equation is applied to each magnetopause data point). This Walén relation test is applied to each data point across the magnetopause window to provide a precise selection of the data that show a reconnection jet. The window of the magnetopause crossing is defined by a transition in density and ion energy flux from data in between the magnetosheath and magnetosphere reference points.

Both the magnetosheath and magnetosphere reference points are selected by visual consideration of the data of each satellite in each event for a stable and representative period. The reference periods must have limited variations in plasma density, plasma β, plasma velocity and magnetic fields. The magnetosheath reference period is chosen to be within about 10 min of the magnetopause crossing and show no signs of magnetospheric plasma in the ion spectra. This ensures the reference period data is from plasma that is incident on the magnetopause at the location of spacecraft crossing. The magnetosheath reference period typically has a density above 10 cm^{-3}. In addition, the peak ion energy flux in the magnetosheath reference period is a few keV whereas in the magnetosphere is 10's of keV. Each reference period is calculated as an average of 5 sequential data points, about 15 s.

Some events showed large variability and outliers in the anisotropy factor in the magnetopause window which affects the outcomes of the Walén relation. The plasma pressures used to calculate the anisotropy factor come from the total (ion and electron) plasma temperature and density which are calculated data products from the plasma moments (McFadden et al., 2008). A possible source of erroneous values in the anisotropy factor is from compounding error in the multiple instruments and calculations required for the anisotropy factor. On the infrequent occurrence that a data point's calculated α was less than -10 or more than 0.75, it was limited to -10 or 0.75 respectively to decrease the outlier's impact on the outcome of the Walén relation.

In addition to the theoretical velocity enhancement provided by Equation 1, the Walén relation requires comparison to an observed plasma velocity. $\Delta\vec{V}_{observed}$ is the plasma velocity difference between each magnetopause point, subscript 2 and magnetosheath reference point subscript 1, Equation 3.

$$\Delta\vec{V}_{observed} = \vec{V}_2 - \vec{V}_1 \tag{3}$$

The presence of a reconnection jet is evaluated by comparing scalar, non-dimensional numbers from the Walén test and observations. For example, Phan et al. (2013) and Zou et al. (2020) use ΔV^*, defined in Equation 4 as the magnitude comparison of the velocity enhancement. In addition, Trenchi et al. (2008) used Θ^*, defined below in Equation 5 to compare the angle between the theoretical and observed jet directions. These parameters are evaluated at every data point through the magnetopause to define an instance of valid reconnection jet observation.

$$\Delta V^* = \frac{\Delta\vec{V}_{theoretical} \cdot \Delta\vec{V}_{observed}}{\left|\Delta\vec{V}^2_{theoretical}\right|} \tag{4}$$

and

$$\Theta^* = \arccos\frac{\Delta\vec{V}_{theoretical} \cdot \Delta\vec{V}_{observed}}{\left|\Delta\vec{V}_{theoretical}\right| \cdot \left|\Delta\vec{V}_{observed}\right|} \tag{5}$$

To put constraints on the theoretical and observed comparison, Trenchi et al. (2008) uses $0° < \Theta^* < 30°$, and $150° < \Theta^* < 180°$ for observations north or south of the reconnection site. The plasma flow direction may present as positive or negative depending on the location of the spacecraft with respect to the X-line, therefore Θ^* conditions must account for this with a two sided constraint. Phan et al. (2013), Zou et al. (2019) and Zou et al. (2020), consider $\Delta V^* > 0.5$ as a reconnection event, as values of ΔV^* closer to 1 mean better agreement with theory. Previous studies find the value of ΔV^* trends below 1, near 0.8, and the condition must allow for this (Vines et al., 2015).

The analysis conducted in this paper requires the conditions of $0° < \Theta^* < 30°$, or $150° < \Theta^* < 180°$ as well as $\Delta V^* > 0.5$, identical to previous studies, in addition with the condition of ion plasma velocity greater than 50 km/s and ion plasma density greater than 3 cm^{-3} as to not extend into the magnetosphere, earthward of the magnetopause. Additionally, the analysis only considers a passing Walén relation if 2 out of 3 sequential data points pass the numerical constraints.

The Walén relation is used to provide a consistent comparison metric between crossings. Extreme care has been taken when selecting the critical magnetosheath reference time, but instances occur where visually the data show signs of reconnection, (i.e., velocity enhancements) and the Walén relation conditions do not consider the event a reconnecting magnetopause. Only the events that meet the Walén relation velocity enhancement comparison conditions stated in the previous paragraph are considered reconnection events.

There are four possible scenarios resulting after the Walén relation is applied to each event of two spacecraft crossing the magnetopause:

1. Both spacecraft measure a reconnection jet near simultaneously, **less** than 1 min apart
2. Both spacecraft measure a reconnection jet not simultaneously, **more** than 1 min apart
3. Only one spacecraft observes a reconnection jet
4. Neither spacecraft observes a reconnection jet

The 1 min allowance was decided upon based on previously published reconnection spreading speeds. Zou et al. (2018) experimentally determined the spreading speed as a few 10's of km/s at the magnetopause with several observations including spacecraft and auroral measurements. Additionally, models of the magnetopause find X-line spreading speed near 70 km/s (Y. Chen et al., 2020). In the statistical study, the mean of all events less than 8,000 km spacing is 3,540 km (Figure 2). The time for a reconnection X-line to spread 3,540 km is 44 s when estimating an average spreading speed near 80 km/s, the upper limits of Zou et al. (2018) and higher than Y. Chen et al. (2020). This resulted in the definition of a 1 min allowance for simultaneous jet observations between satellites.

The second possible outcome from the Walén relation, is if both satellites measure a reconnection jet, but not simultaneously, more than 1 min apart. Although both spacecraft could be measuring a jet from one spatially continuous X-line, it cannot be guaranteed due to the lack of temporal information.

The third and fourth scenarios are if only one or neither spacecraft observe a reconnection jet. These four types of events are collected and binned for comparison.

2.3. Case Study 1: One Satellite Observes Reconnection, One Does Not

The first case study presents an example when one THEMIS satellite observes active reconnection and the other does not when they are both crossing the magnetopause. Figure 3 displays a magnetopause crossing of the THEMIS-C (THC) and THEMIS-D (THD) satellites on 8 August 2008 at 15:45 UT. Panels a–d show THC magnetic field, ion velocity, ion density and ion energy flux. Panels e–h show the same quantities for THD. Reference times, selected for the analysis of the crossing are marked in the black vertical lines.

At the time of the crossing, the spacecraft were separated by 36,918 km (5.8 Re). The spacecraft orbits are shown on the right in panels i and j. Spacecraft position during magnetopause observation time is marked with a star. The coordinate system is GSM. THC experiences multiple magnetopause crossings, due to the motion of the magnetopause along the spacecraft orbit, and did not observe a reconnection jet. At the time of the simultaneous crossing to THD (15:45), THC observed a ΔV^* of 0.55, which is above the condition of 0.5, but the Θ^* was 34.3°, which is larger than the 30° requirement. At this time the ion plasma velocity magnitude was only 70.2 km/s.

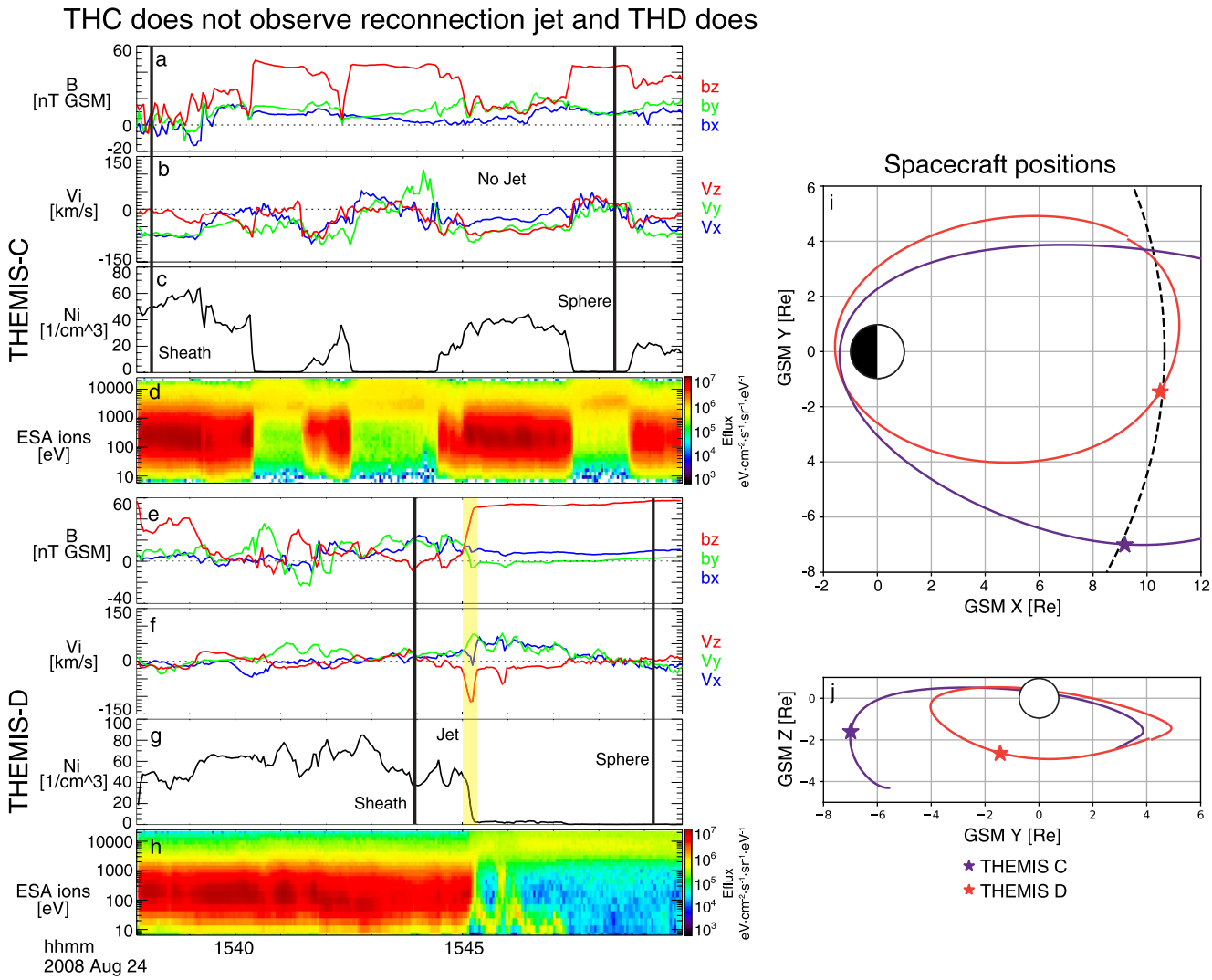

Figure 3. Magnetopause crossing of THEMIS-C (THC) and THEMIS-D (THD) on 8 August 2008. Panels (a–d) and (e–h); magnetic field, ion plasma velocity, ion density and ion energy flux of THC and THD respectively. Coordinate system is GSM. Sheath reference time interval, average of 5 data points, (15 s) for Walén analysis is shown with the black vertical *Sheath* line. The *Sphere* vertical line is a reference time used for shear analysis. The yellow highlight shows the location of the reconnection jet. Panels (i, j) show the spacecraft orbits with a modeled magnetopause.

THC does observe an enhancement in the GSM Y velocity, though this is could be attributed to the magnetopause motion along the spacecraft track.

By contrast, closer to the sub-solar point, THD did observe a reconnection jet when crossing from the magnetosheath into the magnetosphere. During a 27 s window that passed the Walén relation conditions, ΔV^* reached a maximum of 0.94 with a minimum plasma velocity direction difference of 6.4°. The enhancement of the GSM Z plasma velocity shows the spacecraft is south of the X-line.

2.4. Case Study 2: Both Satellites Observe Reconnection Simultaneously, Within 1 min of Each Other

Case study 2 presents a time period when two spacecraft were present at the magnetopause and both observe signatures of reconnection. Figure 4 shows a magnetopause crossing of the THD and THEMIS-E (THE) satellites on 7 October 2009 at 19:30 UT. Layout of the figure's panels are identical that of Figure 3. In this event both spacecraft cross from the magnetosheath into the magnetosphere and observe northward directed reconnection jets, indicating both spacecraft are above (+Z) the X-line. At the time of the magnetopause crossing, the spacecraft were separated by 3,954 km (0.62 Re).

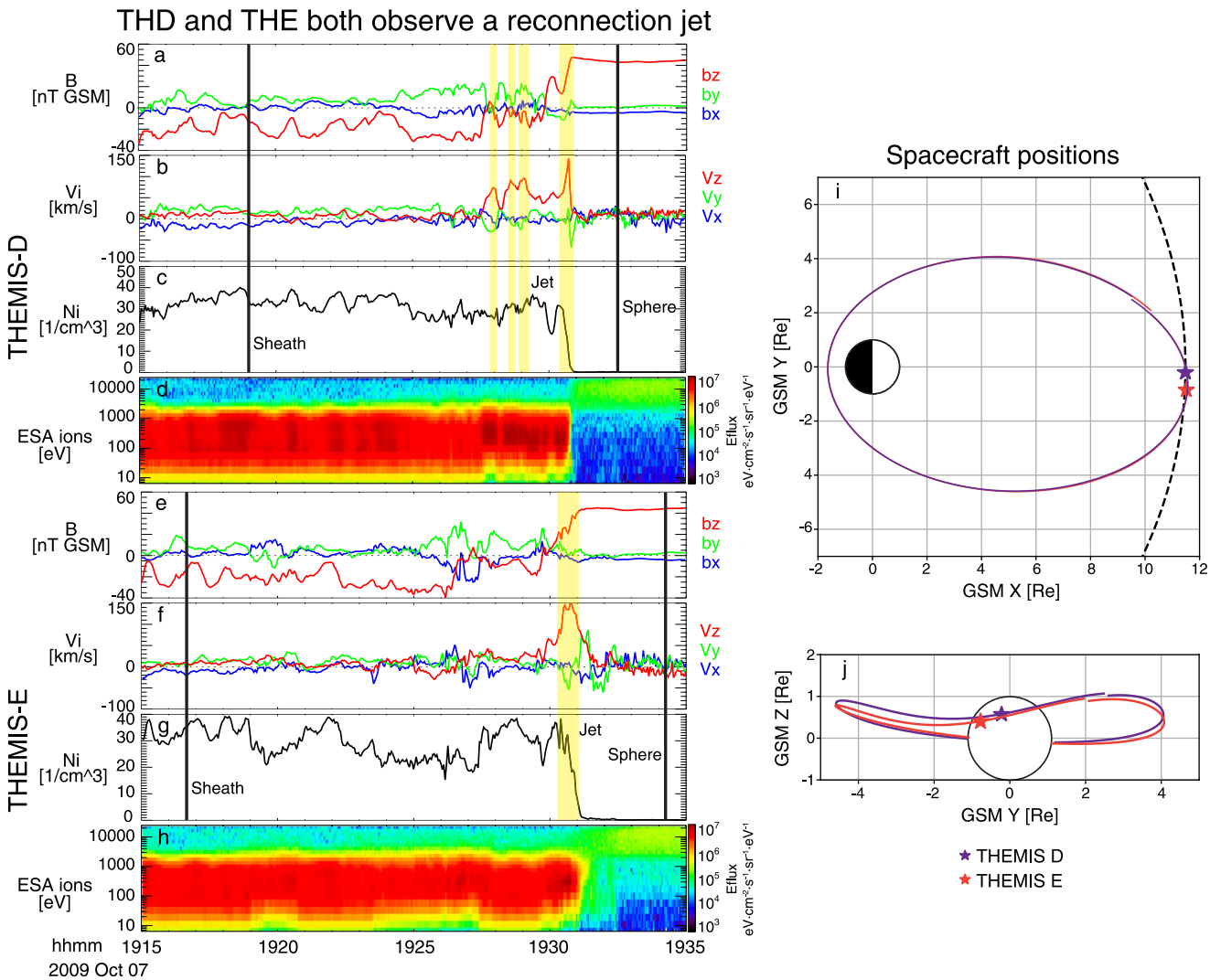

Figure 4. Magnetopause crossing of THA and THEMIS-E (THE) on 7 October 2009. Similar to Figure 3, panels (a–d) and (e–h); magnetic field, ion plasma velocity, ion density and ion energy flux of THA and THE respectively. Coordinate system is GSM. The yellow highlight shows the location of the reconnection jet. Panels (i, j) show the spacecraft positions with respect to magnetopause model.

THD detected multiple encounters with a reconnection jet. During the jet of maximum GSM Z velocity, 129 km/s, the ΔV^* was 0.64 and the difference in jet direction, Θ^* was 23.3°. THE also detected a reconnection jet which produced a ΔV^* of 0.67 and minimum Θ^* of 15.4° at the time of the jet. Both data sets show sustained ΔV^* and Θ^* parameters for multiple data points, therefore passing the Walén relation conditions.

Two of the outcome scenarios described at the end of Section 2.2 include both spacecraft observing reconnection jets. Two satellites measuring reconnection jets greater than 1 min apart may not be observing one contiguous X-line. Figure 5 shows a bar plot of two spacecraft reconnection jet timing observations. A majority of the observations, 74, are within 30 s of each other. Figure 4 is in this category. Only 10 observations are separated by a time between 30 s and 1 min. Few observations exist above 1 min because the event selection process, described in Section 2.1 limits these events. Additionally, there are some events in which the Walén relation is applied to larger windows (>3 min) and multiple crossings (the magnetopause is moving to and away from the satellite) when some crossings show signs of a jet and others do not.

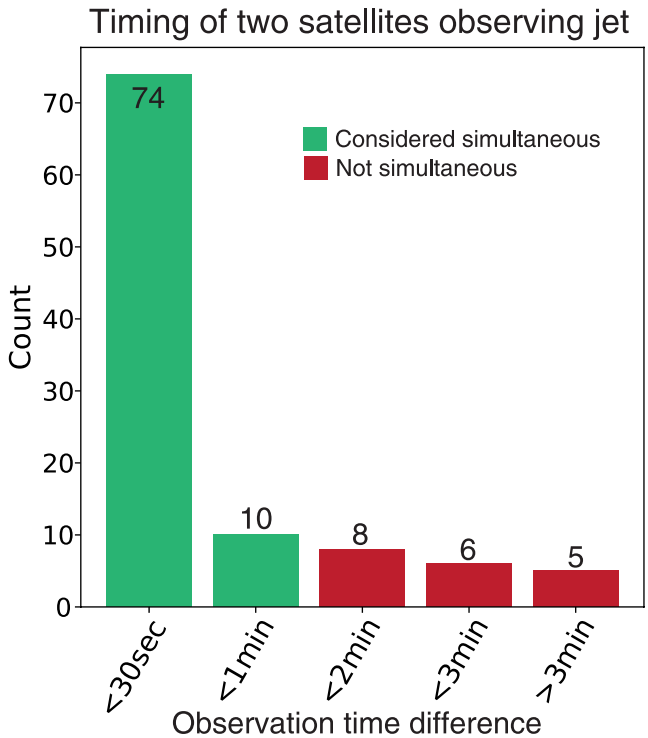

Figure 5. Timing of satellite reconnection jet observations. Jet observation timing less than 1 min is considered simultaneous (green) whereas observations greater than 1 min are not simultaneous (red).

3. Statistical Results

Results from the 174 events with spacing less than 8,000 km (blue histogram in Figure 2) are separated into one of the four possible scenarios. Figure 6 reports the results in these categories along with Gaussian fit to the data for a mean measurement. Calculations of the mean are also included. The bin size of the histograms is 1,000 km. 84 of the 174 events are of satellites in which both observe reconnection jets less than 1 min apart, Figure 6a. Figure 6b shows the 19 events in which both satellites measure reconnection jets, but more than 1 min apart, considered non-simultaneous. These 19 events are the events colored red in 5. Scenarios in which only one or neither satellite observes are reconnection jet is shown in Figures 6c and 6d.

The mean inter-spacecraft distance of the scenario of both satellites observing reconnection simultaneously is the minimum of all four scenarios.

Figure 7 compares the satellite spacing distribution for simultaneous X-line observation events with that of the union of the other event types. Green bars with the purple Gaussian fit show simultaneous events whereas orange bars with the red Gaussian fit show the other event types. Figure 7 plots all 174 events, and shows that the mean event spacing for simultaneous events (3,148 km) is less than the mean of the combined other events (3,906 km).

A Welch's T-test with a P value below 1% means the conclusion is statistically significant and the null hypothesis can be rejected. Rejection of the null hypothesis means these data sets come from distinct, larger populations with different means. The Welch's T-test on the simultaneous event and combined other events reports a T value of 2.9 and a P value of 0.42%. This indicates that simultaneous reconnection observations are more likely to occur the closer spacecraft are. A possible reason for this conclusion is that local magnetosheath properties or LT position may play a role in limiting further reconnection extent.

4. Reconnection Suppression Conditions

As reconnection is thought to sometimes be a process that extends across a wide extent along the magnetopause, a logical question to investigate next is; are there physical processes inhibiting reconnection at spacecraft locations where a reconnection jet is not observed? One proposed process is the relationship between the change in plasma beta ($\Delta\beta$, where β is the ratio of plasma pressure to magnetic pressure) and magnetic shear angle (θ) across the discontinuity. Swisdak et al. (2003); Swisdak et al. (2010) defined the relationship shown in Equation 6.

$$\Delta\beta < 2(L/\lambda_i)\tan(\theta/2) \tag{6}$$

L is the width of the current sheet adjusted by λ_i, the ion skin depth. The width L, although a free parameter, is typically on the scale of the ion diffusion region, which is comparable to λ_i. Therefore L/λ_i is estimated between 0.5 and 2. Phan et al. (2013) conducted a statistical study of 91 single THEMIS spacecraft crossing the magnetopause using the diamagnetic suppression Swisdak et al. (2003, 2010) relationship in Equation 6. Combined with the Walén relation to determine the presence of a reconnecting magnetopause, Phan et al. (2013) found positive agreement with the $\Delta\beta$–θ model. Trenchi et al. (2015) also found positive agreement with the $\Delta\beta$–θ model focusing on jet reversals, in which the spacecraft observes both sides of the X-line. The $\Delta\beta$–θ relationship has also shown positive results at Saturn's magnetopause, making it a versatile metric by which reconnection can be possible (Fuselier et al., 2014; Masters et al., 2012).

Discrepancies between theory and observation do occur where, for example, the $\Delta\beta$–θ relationship predicts reconnection is possible, but a satellite measurement does *not* show a reconnection jet (Phan et al., 2011; Trenchi et al., 2015; Zou et al., 2020), or vice versa. One possibility of this inconsistency is because single point satellite measurements of sheath properties do not show the larger perspective of the $\Delta\beta$–θ relationship that could be

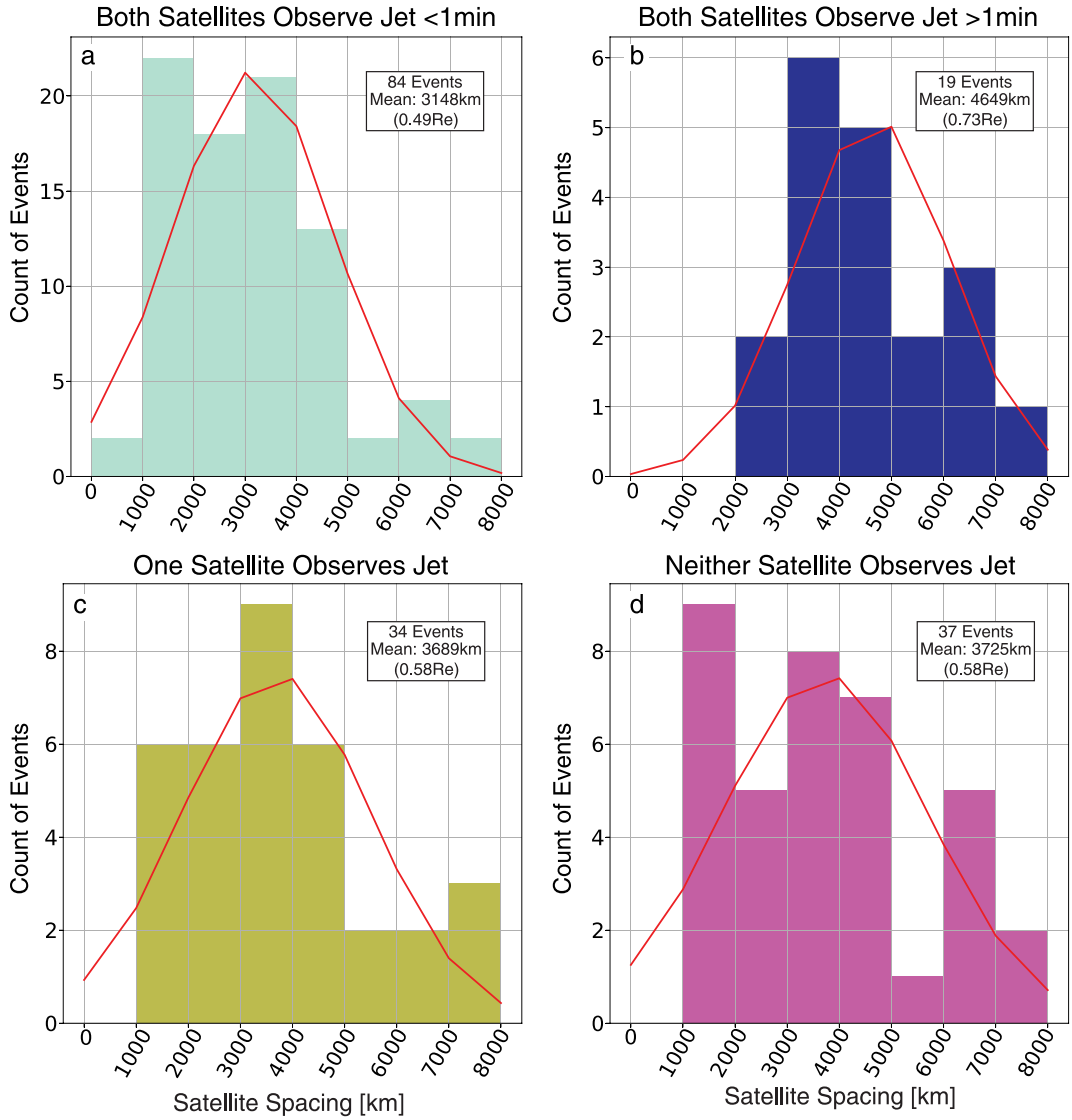

Figure 6. Histograms of the four possible scenarios resulting from the Walén relation. Bin size is 1,000 km. (a) Both satellites measure reconnection jets simultaneously, Figure 4 is considered in this category. (b) Both satellite observe a reconnection jet, though not simultaneously. (c) Only one satellite measures reconnection. (d) Neither satellite observes a reconnection jet.

driving the reconnection elsewhere. A satellite may be some distance from the X-line and still observe a reconnection jet although local properties at the satellite suggest suppression. Single crossings may be outliers, but large statistics aid in defining an accurate mean for $\Delta\beta$–θ relationship.

In the data set presented in this paper, the β and θ values are calculated from the magnetosheath and magnetosphere reference times, averages of five data points, or 15 s. Example locations of the reference times are found in Figures 3 and 4. Figure 8 compares the instances of reconnection jet observations (A, blue, top left) versus that of no jet observations (B, black, bottom left). Figure 8 considers each satellite magnetopause crossing individually, regardless of event type. The error bars are the standard deviation of the data used to generate the values divided by the number of data points. Figure 8c shows the combination of the reconnecting and not reconnecting magnetopause observations, and the appropriate means for the data sets. Although there are instances which do not agree with the Swisdak et al. (2003) relationship, the means agree surprisingly well.

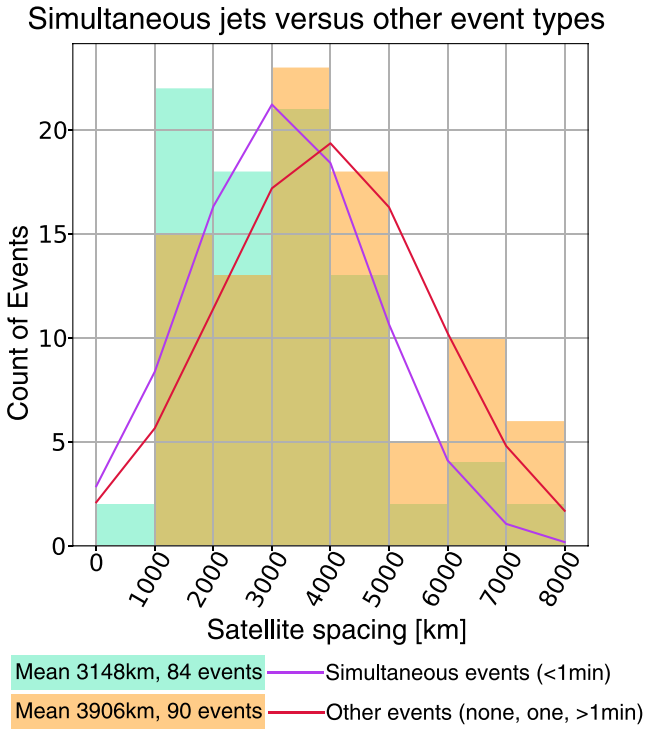

Figure 7. Comparison of two satellites observing simultaneous reconnection jets to other event types, non-simultaneous, one satellite and neither satellite jet observations.

5. Reconnection Spatial Limitations

Varying critical reconnection properties such as $\Delta\beta{-}\theta$ and dependence on current sheet thickness further begs the question, does the spatial extent of reconnection preferentially terminate down the magnetopause flanks? At local noon, the sub solar point is likely compressed from the magnetosheath flow providing a thinner current sheet for reconnection to persist at varying magnetic shear conditions. Whereas along the flanks, both theory and observations predict a thicker boundary layer or current sheet (Haaland et al., 2014) which may suppress reconnection. This phenomenon has been proposed from spacecraft observations and analysis of the $\Delta\beta{-}\theta$ dependence (Phan et al., 2013). Diamagnetic suppression has been shown to turn off reconnection, thus limiting it spatially (Trenchi et al., 2015). PIC models have shown reconnection to spread at slower rates when the current sheet is thicker (Li et al., 2020). Thick current sheets in night-side PIC models are used to confine reconnection extent (Liu et al., 2019), although it has been shown that simulation size can affect spreading properties of varying current sheet thickness in a two-fluid code (Arencibia et al., 2021).

If current sheet thickness or shear flow may inhibit reconnection spreading, then examining the LT relationship of events in which only one spacecraft observes reconnection may be illuminating. We calculate the LT angle off of noon for each satellite (i.e., local noon is 0°, dawnward is negative and duskward is positive). The difference between the LT of a satellite that does not observe reconnection to the LT of a satellite that does is given by Equation 7. Should this value trend positive, it would be consistent with the prediction that reconnection initiates near the sub-solar region terminates toward the flanks.

$$\Delta LT = |LT_{noRx}| - |LT_{yesRx}| \tag{7}$$

Equation 7 is applied to the events of one out of two spacecraft observe a reconnection jet. For the 34 events below 8,000 km used in the statistical analysis, $\Delta LT = -0.015°$. This value close to 0 shows that with small spacecraft spacing, (average of the data is 0.58 Re) reconnection does not preferentially terminate toward the flank. This can likely be attributed to convection of the X-line around the magnetopause, with dependence on when the spacecraft cross the magnetopause to make the observation.

Equation 7 is also applied to the nine events greater than 8,000 km (mean of 32,851 km) with only one out of two spacecraft observing reconnection. Figure 3 is considered in this category. The result, is $\Delta LT = 8.8°$. Eight out of the nine events have the flank-ward satellite not observe reconnection. The event shown in Figure 3 fits this criteria. This larger, positive value means reconnection, as observed by THEMIS, does preferentially terminate further from local noon, possibly due to shear flow or current sheet thickness.

6. Conclusions

In this work, we use a statistical study to classify magnetopause reconnection scenarios and conditions that may inhibit reconnection. THEMIS orbits were analyzed for magnetopause crossings from 2008 to 2010. Crossing times of a THEMIS satellite which coincided with another THEMIS satellite (conjunction events) were further analyzed for the presence of reconnection with the Walén relation. The 208 events were limited to 174 events by a 8,000 km satellite spacing condition because of low statistics above 8,000 km. The 174 events were binned into four separate categories; simultaneous (<1 min), non-simultaneous (>1 min), single satellite and neither satellite reconnection observation. The 84 simultaneous observations, compared to the other three event types (counts of 19, 34, and 37 respectively, and total 90), shows statistical significance coming from different, larger populations.

The event analysis leads to two conclusions. First, we conclude that two satellites are more likely to observe reconnection the closer they are spatially. The 84 simultaneous reconnection jet observations have a mean spacecraft spacing of 3,148 km, meaning that magnetopause reconnection is at least this long spatially.

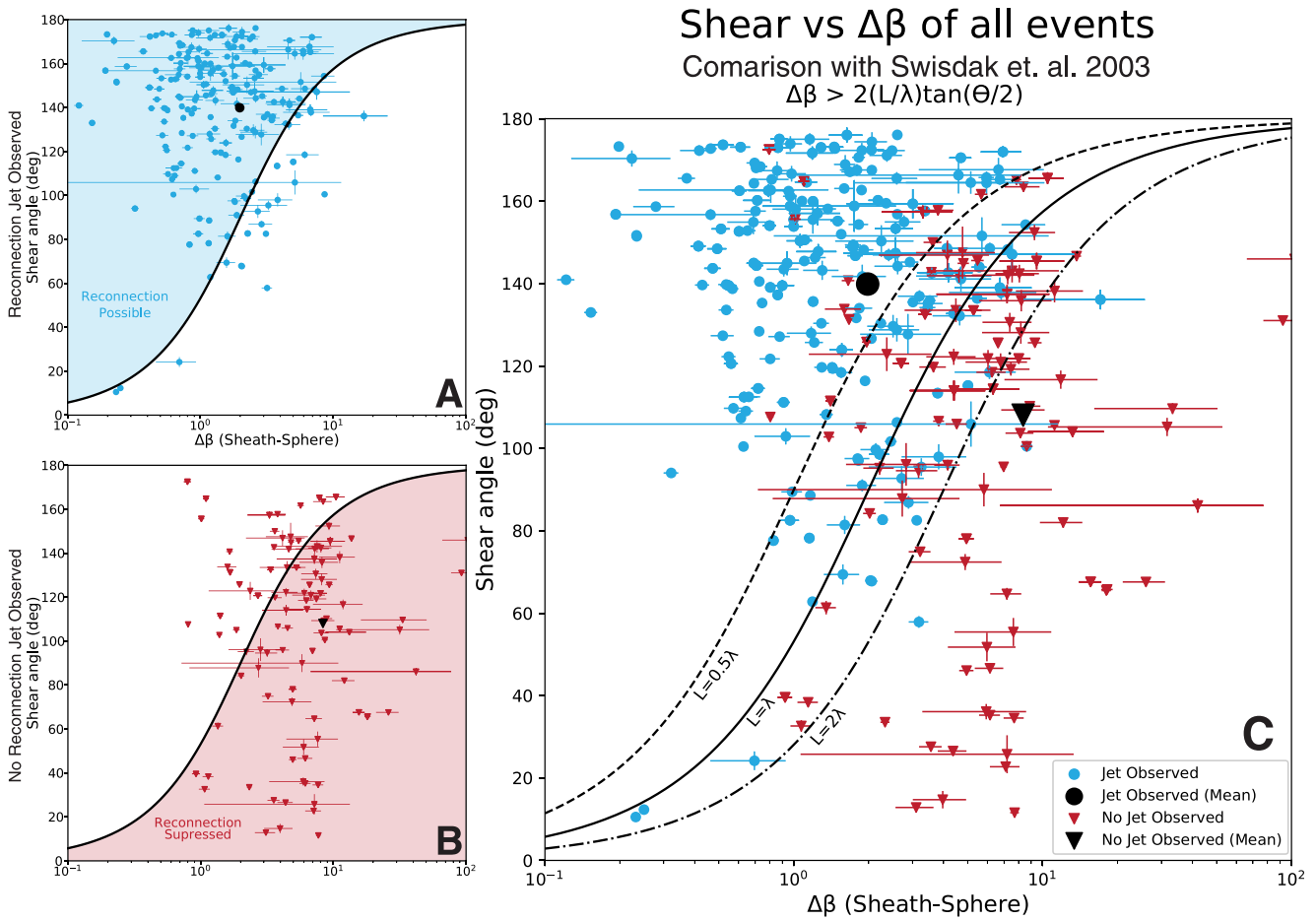

Figure 8. $\Delta\beta$–θ relationship of the analyzed data set. (a) $\Delta\beta$–θ of spacecraft that **did** observe a jet. (b) $\Delta\beta$-θ of spacecraft that **did not** observe a jet. (c) Combined jet and non-jet crossings. Theoretical limitations, black curves are given from Swisdak et al. (2003). Error bars are the standard error from the β calculation and magnetic field (θ).

Second, we conclude that reconnection is not always extended across the entire magnetopause. Forty three events show reconnection jets at only one satellite while a second satellite fails to observe active reconnection. Additionally, there is a preference for the THEMIS spacecraft to not observe reconnection further away from the sub-solar region. This is not to say reconnection is never extended, but that reconnection can be spatially localized *or* extended, further supporting an expanding X-line model. Analysis of the $\Delta\beta$–θ relationship for reconnection suppression, in which high plasma $\Delta\beta$ inhibits reconnection even for large magnetic shear, θ, shows good agreement with theory for the 208 events. This reinforces the concept that varying local $\Delta\beta$ and θ may inhibit reconnection extending to larger scales, and prevent reconnection from traveling down the magnetopause flanks.

Data Availability Statement

The data used for this research can be accessed from: http://themis.ssl.berkeley.edu/data/themis/.

Acknowledgments
The authors would like to thank the THEMIS team. We acknowledge NASA contract NAS5-02099 and V. Angelopoulos for use of data from the THEMIS Mission. Specifically: C. W. Carlson and J. P. McFadden for use of ESA data and K. H. Glassmeier, U. Auster and W. Baumjohann for the use of FGM data. FGM data provided under the lead of the Technical University of Braunschweig and with financial support through the German Ministry for Economy and Technology and the German Center for Aviation and Space (DLR) under contract 50 OC 0302. The authors of this work were supported by NASA Grant NNX16AJ73G, Heliophysics Technology and Instrument Development for Science program and NSF Grant 1845151.

References

Angelopoulos, V. (2009). The THEMIS mission. In *The THEMIS mission* (pp. 5–34). Springer.

Arencibia, M., Cassak, P. A., Shay, M. A., & Priest, E. R. (2021). Scaling theory of three-dimensional magnetic reconnection spreading. *Physics of Plasmas*, *28*(8), 082104. https://doi.org/10.1063/5.0052189

Auster, H., Glassmeier, K., Magnes, W., Aydogar, O., Baumjohann, W., Constantinescu, D., et al. (2008). The THEMIS fluxgate magnetometer. *Space Science Reviews*, *141*(1), 235–264. https://doi.org/10.1007/s11214-008-9365-9

Burch, J., & Phan, T. (2016). Magnetic reconnection at the dayside magnetopause: Advances with MMS. *Geophysical Research Letters*, *43*(16), 8327–8338. https://doi.org/10.1002/2016gl069787

Chen, L.-J., Hesse, M., Wang, S., Gershman, D., Ergun, R., Pollock, C., et al. (2016). Electron energization and mixing observed by MMS in the vicinity of an electron diffusion region during magnetopause reconnection. *Geophysical Research Letters*, *43*(12), 6036–6043. https://doi.org/10.1002/2016gl069215

Chen, Y., Toth, G., Hietala, H., Vines, S., Zou, Y., Nishimura, Y., et al. (2020). Magnetohydrodynamic with embedded particle-in-cell simulation of the geospace environment modeling dayside kinetic processes challenge event. arXiv preprint arXiv:2001.04563.

Chisham, G., Freeman, M. P., Abel, G. A., Lam, M. M., Pinnock, M., Coleman, I. J., et al. (2008). Remote sensing of the spatial and temporal structure of magnetopause and magnetotail reconnection from the ionosphere. *Reviews of Geophysics*, *46*(1), RG1004. https://doi.org/10.1029/2007RG000223

Dunlop, M., Zhang, Q.-H., Bogdanova, Y., Lockwood, M., Pu, Z., Hasegawa, H., et al. (2011). Extended magnetic reconnection across the dayside magnetopause. *Physical Review Letters*, *107*(2), 025004. https://doi.org/10.1103/physrevlett.107.025004

Eriksson, S., Wilder, F., Ergun, R., Schwartz, S., Cassak, P., Burch, J., et al. (2016). Magnetospheric multiscale observations of the electron diffusion region of large guide field magnetic reconnection. *Physical Review Letters*, *117*(1), 015001. https://doi.org/10.1103/physrevlett.117.015001

Fear, R., Milan, S., Lucek, E., Cowley, S., & Fazakerley, A. (2010). Mixed azimuthal scales of flux transfer events. In *The cluster active archive* (pp. 389–398). Springer.

Frey, H. U., Han, D., Kataoka, R., Lessard, M. R., Milan, S. E., Nishimura, Y., et al. (2019). Dayside aurora. *Space Science Reviews*, *215*(8), 1–32. https://doi.org/10.1007/s11214-019-0617-7

Fuselier, S., Frahm, R., Lewis, W., Masters, A., Mukherjee, J., Petrinec, S., & Sillanpaa, I. (2014). The location of magnetic reconnection at Saturn's magnetopause: A comparison with earth. *Journal of Geophysical Research: Space Physics*, *119*(4), 2563–2578. https://doi.org/10.1002/2013ja019684

Fuselier, S., Frey, H., Trattner, K., Mende, S., & Burch, J. (2002). Cusp aurora dependence on interplanetary magnetic field B_z. *Journal of Geophysical Research*, *107*(A7), SIA–6. https://doi.org/10.1029/2001ja900165

Fuselier, S., Klumpar, D., & Shelley, E. (1991). Ion reflection and transmission during reconnection at the Earth's subsolar magnetopause. *Geophysical Research Letters*, *18*(2), 139–142. https://doi.org/10.1029/90gl02676

Fuselier, S., Vines, S., Burch, J., Petrinec, S., Trattner, K., Cassak, P., et al. (2017). Large-scale characteristics of reconnection diffusion regions and associated magnetopause crossings observed by MMS. *Journal of Geophysical Research: Space Physics*, *122*(5), 5466–5486. https://doi.org/10.1002/2017ja024024

Genestreti, K., Burch, J., Cassak, P., Torbert, R., Ergun, R., Varsani, A., et al. (2017). The effect of a guide field on local energy conversion during asymmetric magnetic reconnection: MMS observations. *Journal of Geophysical Research: Space Physics*, *122*(11), 11–342. https://doi.org/10.1002/2017ja024247

Genestreti, K. J., Varsani, A., Burch, J. L., Cassak, P. A., Torbert, R. B., Nakamura, R., et al. (2018). MMS observation of asymmetric reconnection supported by 3-D electron pressure divergence. *Journal of Geophysical Research: Space Physics*, *123*(3), 1806–1821. https://doi.org/10.1002/2017ja025019

Haaland, S., Reistad, J., Tenfjord, P., Gjerloev, J., Maes, L., DeKeyser, J., et al. (2014). Characteristics of the flank magnetopause: Cluster observations. *Journal of Geophysical Research: Space Physics*, *119*(11), 9019–9037. https://doi.org/10.1002/2014ja020539

Hoilijoki, S., Ganse, U., Pfau-Kempf, Y., Cassak, P. A., Walsh, B. M., Hietala, H., et al. (2017). Reconnection rates and X line motion at the magnetopause: Global 2D-3V hybrid-Vlasov simulation results. *Journal of Geophysical Research: Space Physics*, *122*(3), 2877–2888. https://doi.org/10.1002/2016ja023709

Hudson, P. (1970). Discontinuities in an anisotropic plasma and their identification in the solar wind. *Planetary and Space Science*, *18*(11), 1611–1622. https://doi.org/10.1016/0032-0633(70)90036-x

Li, T. C., Liu, Y.-H., Hesse, M., & Zou, Y. (2020). Three-dimensional X-line spreading in asymmetric magnetic reconnection. *Journal of Geophysical Research: Space Physics*, *125*(2), e2019JA027094. https://doi.org/10.1029/2019JA027094

Liu, Y.-H., Li, T., Hesse, M., Sun, W., Liu, J., Burch, J., et al. (2019). Three-dimensional magnetic reconnection with a spatially confined X-line extent: Implications for dipolarizing flux bundles and the dawn-dusk asymmetry. *Journal of Geophysical Research: Space Physics*, *124*(4), 2819–2830. https://doi.org/10.1029/2019ja026539

Lyon, J. G. (2000). The solar wind-magnetosphere-ionosphere system. *Science*, *288*(5473), 1987–1991. https://doi.org/10.1126/science.288.5473.1987

Masters, A., Eastwood, J., Swisdak, M., Thomsen, M., Russell, C., Sergis, N., et al. (2012). The importance of plasma β conditions for magnetic reconnection at Saturn's magnetopause. *Geophysical Research Letters*, *39*(8), L08103. https://doi.org/10.1029/2012gl051372

McFadden, J., Carlson, C., Larson, D., Ludlam, M., Abiad, R., Elliott, B., et al. (2008). The THEMIS ESA plasma instrument and in-flight calibration. *Space Science Reviews*, *141*(1), 277–302. https://doi.org/10.1007/s11214-008-9440-2

Milan, S., Lester, M., Cowley, S., & Brittnacher, M. (2000). Convection and auroral response to a southward turning of the IMF: Polar UVI, cutlass, and image signatures of transient magnetic flux transfer at the magnetopause. *Journal of Geophysical Research*, *105*(A7), 15741–15755. https://doi.org/10.1029/2000ja900022

Paschmann, G., Papamastorakis, I., Baumjohann, W., Sckopke, N., Carlson, C., Sonnerup, B. Ö., & Lühr, H. (1986). The magnetopause for large magnetic shear: AMPTE/IRM observations. *Journal of Geophysical Research*, *91*(A10), 11099–11115. https://doi.org/10.1029/ja091ia10p11099

Paschmann, G., Sonnerup, B. Ö., Papamastorakis, I., Sckopke, N., Haerendel, G., Bame, S., et al. (1979). Plasma acceleration at the earth's magnetopause: Evidence for reconnection. *Nature*, *282*(5736), 243–246. https://doi.org/10.1038/282243a0

Petrinec, S., & Fuselier, S. (2003). On continuous versus discontinuous neutral lines at the dayside magnetopause for southward interplanetary magnetic field. *Geophysical Research Letters*, *30*(10), 1519. https://doi.org/10.1029/2002gl016565

Phan, T., Kistler, L., Klecker, B., Haerendel, G., Paschmann, G., Sonnerup, B. Ö., et al. (2000). Extended magnetic reconnection at the Earth's magnetopause from detection of bi-directional jets. *Nature*, *404*(6780), 848–850. https://doi.org/10.1038/35009050

Phan, T., Love, T., Gosling, J., Paschmann, G., Eastwood, J., Oieroset, M., et al. (2011). Triggering of magnetic reconnection in a magnetosheath current sheet due to compression against the magnetopause. *Geophysical Research Letters*, *38*(17), L17101. https://doi.org/10.1029/2011gl048586

Phan, T., Paschmann, G., Gosling, J., Oieroset, M., Fujimoto, M., Drake, J., & Angelopoulos, V. (2013). The dependence of magnetic reconnection on plasma β and magnetic shear: Evidence from magnetopause observations. *Geophysical Research Letters*, *40*(1), 11–16. https://doi.org/10.1029/2012gl054528

Pinnock, M., Chisham, G., Coleman, I., Freeman, M., Hairston, M., & Villain, J.-P. (2003). The location and rate of dayside reconnection during an interval of southward interplanetary magnetic field. *Annales Geophysicae*, *21*(7), 1467–1482. https://doi.org/10.5194/angeo-21-1467-2003

Sandholt, P., & Farrugia, C. (2003). Does the aurora provide evidence for the occurrence of antiparallel magnetopause reconnection? *Journal of Geophysical Research*, *108*(A12), 1466. https://doi.org/10.1029/2003ja010066

Shay, M. A., Drake, J. F., Swisdak, M., Dorland, W., & Rogers, B. N. (2003). Inherently three dimensional magnetic reconnection: A mechanism for bursty bulk flows? *Geophysical Research Letters*, *30*(6), 1345. https://doi.org/10.1029/2002GL016267

Shue, J.-H., Song, P., Russell, C., Steinberg, J., Chao, J., Zastenker, G., et al. (1998). Magnetopause location under extreme solar wind conditions. *Journal of Geophysical Research*, *103*(A8), 17691–17700. https://doi.org/10.1029/98ja01103

Sonnerup, B. Ö., Paschmann, G., Papamastorakis, I., Sckopke, N., Haerendel, G., Bame, S., et al. (1981). Evidence for magnetic field reconnection at the Earth's magnetopause. *Journal of Geophysical Research*, *86*(A12), 10049–10067. https://doi.org/10.1029/ja086ia12p10049

Sun, T., Tang, B., Wang, C., Guo, X., & Wang, Y. (2019). Large-scale characteristics of flux transfer events on the dayside magnetopause. *Journal of Geophysical Research: Space Physics*, *124*(4), 2425–2434. https://doi.org/10.1029/2018ja026395

Swisdak, M., Opher, M., Drake, J., & Bibi, F. A. (2010). The vector direction of the interstellar magnetic field outside the heliosphere. *The Astrophysical Journal*, *710*(2), 1769–1775. https://doi.org/10.1088/0004-637x/710/2/1769

Swisdak, M., Rogers, B., Drake, J., & Shay, M. (2003). Diamagnetic suppression of component magnetic reconnection at the magnetopause. *Journal of Geophysical Research*, *108*(A5), 1218. https://doi.org/10.1029/2002ja009726

Trattner, K., Fuselier, S., Petrinec, S., Yeoman, T., Mouikis, C., Kucharek, H., & Reme, H. (2005). Reconnection sites of spatial cusp structures. *Journal of Geophysical Research*, *110*(A4), A04207. https://doi.org/10.1029/2004ja010722

Trenchi, L., Marcucci, M., Pallocchia, G., Consolini, G., Cattaneo, M. B., Di Lellis, A., et al. (2008). Occurrence of reconnection jets at the dayside magnetopause: Double star observations. *Journal of Geophysical Research*, *113*(A7), A07S10. https://doi.org/10.1029/2007ja012774

Trenchi, L., Marcucci, M. F., & Fear, R. (2015). The effect of diamagnetic drift on motion of the dayside magnetopause reconnection line. *Geophysical Research Letters*, *42*(15), 6129–6136. https://doi.org/10.1002/2015gl065213

Vines, S. K., Fuselier, S. A., Trattner, K. J., Petrinec, S. M., & Drake, J. F. (2015). Ion acceleration dependence on magnetic shear angle in dayside magnetopause reconnection. *Journal of Geophysical Research: Space Physics*, *120*(9), 7255–7269. https://doi.org/10.1002/2015ja021464

Walsh, B., Komar, C., & Pfau-Kempf, Y. (2017). Spacecraft measurements constraining the spatial extent of a magnetopause reconnection x line. *Geophysical Research Letters*, *44*(7), 3038–3046. https://doi.org/10.1002/2017gl073379

Walsh, B., Phan, T., Sibeck, D., & Souza, V. (2014). The plasmaspheric plume and magnetopause reconnection. *Geophysical Research Letters*, *41*(2), 223–228. https://doi.org/10.1002/2013gl058802

Zou, Y., Walsh, B., Nishimura, Y., Angelopoulos, V., Ruohoniemi, J., McWilliams, K., & Nishitani, N. (2019). Local time extent of magnetopause reconnection using space–ground coordination. *Annales Geophysicae*, *37*(2), 215–234. https://doi.org/10.5194/angeo-37-215-2019

Zou, Y., Walsh, B. M., Atz, E., Liang, H., Ma, Q., & Angelopoulos, V. (2020). Azimuthal variation of magnetopause reconnection at scales below an Earth radius. *Geophysical Research Letters*, *47*(4), e2019GL086500. https://doi.org/10.1029/2019GL086500

Zou, Y., Walsh, B. M., Nishimura, Y., Angelopoulos, V., Ruohoniemi, J. M., McWilliams, K. A., & Nishitani, N. (2018). Spreading speed of magnetopause reconnection X-lines using ground-satellite coordination. *Geophysical Research Letters*, *45*(1), 80–89. https://doi.org/10.1002/2017gl075765